

NUMERICAL ASPECTS OF THE STUDY OF THE REGIONAL THERMAL IMPACT OF A RADIOACTIVE WASTE REPOSITORY

J.C. FERRERI * and M.A. VENTURA *

Comisión Nacional de Energía Atómica, Av. del Libertador 8250, 1429 Buenos Aires, Argentina

Received 7 May 1984

Numerical results are obtained for the regional thermal history of a radioactive waste repository. For such a purpose, an alternating direction implicit method has been used, with special treatment of singularities in heat generation, with a variable grid calculation. The results obtained are in accordance with previous results in calibration cases. These results show that the technique developed constitutes a valuable tool for the handling of problems such as the one under consideration. Its application is exemplified by means of a case with a typical geometrical configuration and thermal load.

Introduction

The numerical modelling of the thermal history of a finite mass under thermal loads produced by fission products, called "the repository", introduces interesting difficulties. In order to understand them, we only have to consider the scales associated with the integration domain and those belonging to the heat sources. The overall spatial scales in the area influenced by the repository are of the order of several kilometers and time scale is of the order of thousands of years. On the other hand, the scales corresponding with the sources are of the order of one meter and of hundreds of years, the latter being due to radioactive decay. Fig. 1 illustrates the typical geometry [10].

Consideration must be given to the three-dimensional computational grid (3D) aimed at studies that follow this paper, consisting of predicting the water flow and the diffusion of radionuclides toward the surface. This fact, along with the various scales mentioned above, leads to the consideration of heat generation singularities in the heart of the rock if a reasonable number of calculation points (of the order of 2000) is used.

A plenty of literature is now available on semianalytical and numerical studies for cases similar to the one discussed herewith. Among the former, based on the

members of Carrera del Investigador Científico of the Consejo Nacional de Investigaciones Científicas y Tecnológicas (CONICET), Argentina.

analysis of the thermal problem involving the exclusive use of singularities for the approximate description of the problem, we may quote refs. [3,14,18]. Among the latter, we may quote refs [1,2,5,16,17].

Ratigan [12], Thunvik [13] and Rae and Robinson [11] described calibration work aimed at validating the results obtained for finite elements in the case of heat conduction and liquid movement. In these cases, the number of nodes involved for the calculations is of the order of 400 for plane symmetry, which allows us to assume an order of 16000 nodes for the non-symmetrical 3D case.

Considering the need to maintain the CPU time necessary for simulation within a given margin, in turn implying the reduction of nodes to the minimum possible number while keeping results accurate, it is important to consider a technique that deals adequately with the presence of the heat sources. As has already been discussed, these sources may be considered as singularities and, for this case, a work by Emery [7] deserves to be taken into account as a technique of interest. Some details of this technique may be found in Appendix A and have only been included for the sake of clarification, since the original technique is employed in a broader sense. Conceptually, this implies considering the local contribution of singularities as a source distributed over the grid, thus discarding the usual difficulty associated with the accuracy of discrete schemes around the almost punctual sources located in isolated points of the grid.

This paper shows the results obtained from associat-

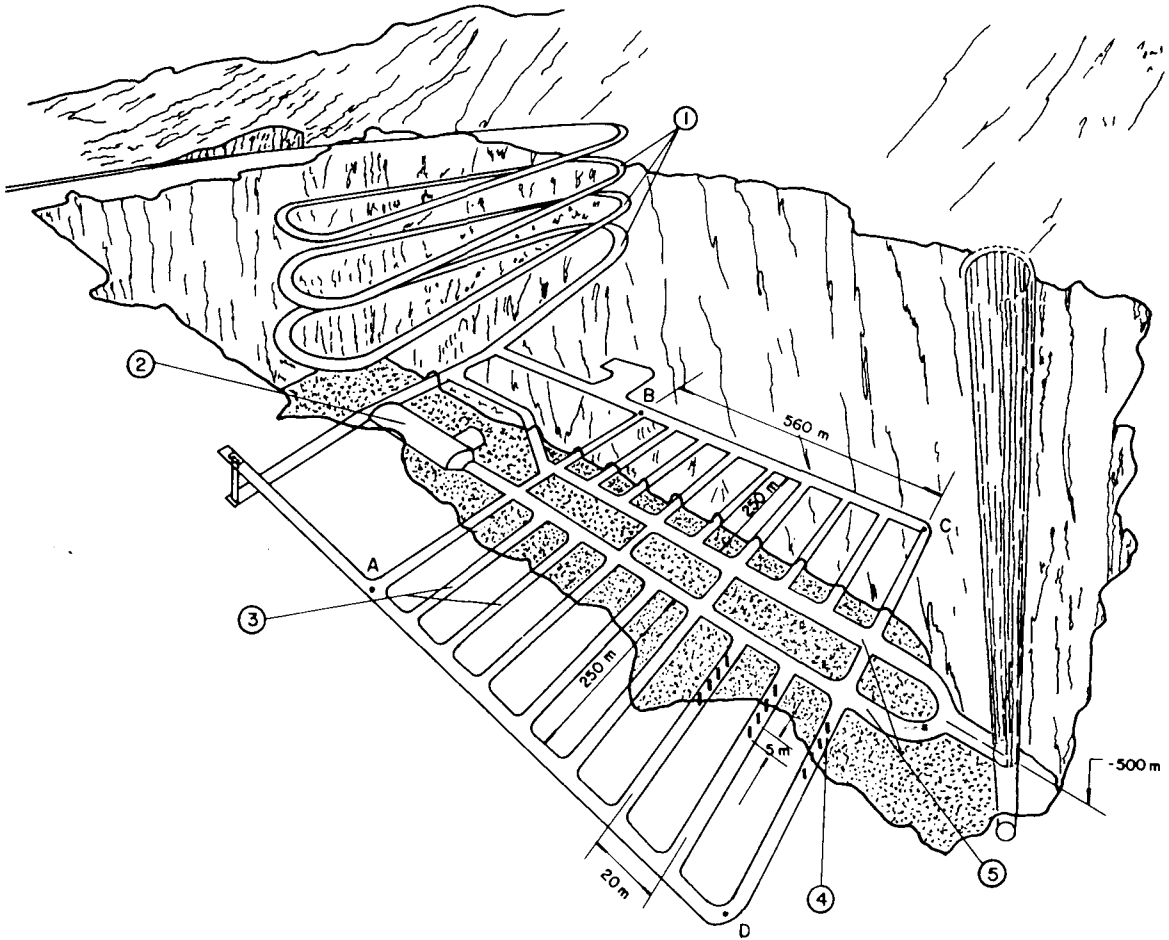


Fig. 1. Idealized repository (out of scale): 1, Access ramp. 2, Service area. 3, Contention galleries. 4, Containers. 5, Main galleries.

ing a generalization of Emery's technique [7] with an alternating direction implicit scheme (ADI) of the D'Yakonov's type (see Marchuk [9]) in cases of interest, applied to the problem of predicting the thermal history of a repository.

The following paragraphs will serve to illustrate the technique developed, the calibration cases and the results obtained for a typical case relating to the projected repository. The results of the complete study, including a parametric study of the repository, will be considered separately from this paper.

2. The numerical technique

As may be seen in Appendix A, the solution of the

problem:

$$\partial T / \partial t = \alpha \nabla^2 T + \sum_i q_i, \quad (1)$$

where T is the local temperature, α is the thermal diffusivity of the rock, t is time and q_i represents i singularities distributed in the heart of the rock, may be obtained from the solution of the problem:

$$\partial T / \partial t = \alpha \nabla^2 T + \sum_i \left(\frac{\partial S_i}{\partial t} - \alpha \nabla^2 S_i \right), \quad (2)$$

where S_i is known, corresponding to the solution of the problem;

$$\partial S_i / \partial t = \alpha \nabla^2 S_i + q_i$$

in the vicinity of singularity.

In discrete terms, eq. (2) must be written as follows:

$$\prod_{i=1}^3 \left(1 - \frac{\Delta t}{2} \alpha \delta_{xi}^2 \right) T_P^{n+1} = \prod_{i=1}^3 \left(1 + \frac{\Delta t}{2} \alpha \delta_{xi}^2 \right) T_P^n + \sum_i \left(S_P^{n+1} - S_P^n - \frac{\Delta t \alpha}{2} (\nabla_h^2 S_P^{n+1} + \nabla_h^2 S_P^n) \right) \equiv TI, \tag{3}$$

where P indicates a generic point in the grid $P(x, y, z)$, $n + 1$ is an indication of time $t = (n + 1)\Delta t$ and subscript h indicates a discrete form of the Laplacian, taken to be the same as that considered for $\nabla^2 T$.

Since the terms involved in the variation of S may be considered as data and are obtained as shown in the following paragraph, eq. (3) is directly treatable as for an ADI scheme like the one considered by Ventura et al. [17], valid for the quasi-linear problem. In this case, however, it was convenient to modify it in order to consider a grid varying in space. The algebraic details are somewhat tedious and only the final results are included here.

When an ADI process is applied, eq. (3) appears as follows:

$$\begin{aligned} \left(1 - \frac{\Delta t}{2} \alpha \delta_x^2 \right) T_P^* &= TI, \\ \left(1 - \frac{\Delta t}{2} \alpha \delta_y^2 \right) T_P^{**} &= T_P^*, \\ \left(1 - \frac{\Delta t}{2} \alpha \delta_z^2 \right) T_P^{n+1} &= T_P^{**}. \end{aligned} \tag{4}$$

The consideration of a variable grid only implies alternating the form of the coefficients in the tridiagonal expression corresponding to the left member in eqs. (4) and to TI . Thus, if one of the equations is:

$$A^- T_{i-1} + A T_i + A^+ T_{i+1},$$

then, the coefficients are expressed as follows:

$$\begin{aligned} A^- &= -\Delta t \alpha / h_1 (h_1 + h_2), \\ A &= 1 - \Delta t \alpha / h_1 h_2, \\ A^+ &= -\Delta t \alpha / h_2 (h_1 + h_2). \end{aligned}$$

In the previous expressions $h_2 = x_{i+1} - x_i$ and $h_1 = x_i - x_{i-1}$. It must be taken into account that the accuracy of the results degrades if h_1 and h_2 are variable and that this must be considered in the evaluation of the same.

The quasi-linear case must be treated in the same way. In this case the algorithm shown in Ventura et al.

[17] may be applied, with an adequate evaluation of the coefficients varying in space.

Some considerations must be made here concerning the code developed. This represents a highly compact algorithm in which the successive steps of the ADI are obtained through the permutation of subindexes. This, along with a library sub-routine for solving tridiagonal systems in linear equations, allowed the results to be obtained with great computational efficiency. The source terms, see section 3, were obtained in some cases from modules separated from the main code.

3. Analysis of certain singularities

As was previously mentioned, the technique applied calls for knowledge of the analytical solution to certain singularities that are representative of the case under analysis. Three singularities are usually found in the cases under study: point sources, finite-length linear sources and plane sources.

The point source is representative of a container, as if the latter were isolated in the rock, since it should not be ignored that it is small if compared with the geometrical scale of the repository. It may be argued that each container may be a source with finite length and radius. However this would imply considering 3000 isolated sources for a typical case, thus discarding the possibilities of application, as will be seen further on in this report. The finite-length linear source is of interest, since it represents a gallery of containers, and a plane source would be of interest if a continuous power distribution had to be simulated.

The integration of the heat transfer equation resulting from the presence of specific features has been described in classical works, such as ref. [6], although it has only recently been applied to cases such as the one analyzed here.

Thus, the equation

$$\partial S / \partial t = \alpha \nabla^2 S, \tag{5}$$

when there is an instantaneous release of a given amount of heat, Q , at a point of coordinates $x'y'z'$, is solved as follows:

$$S = \frac{Q}{4(\pi \alpha t)^{3/2}} \exp \left\{ - \left[(x - x')^2 + (y - y')^2 + (z - z')^2 \right] / 4 \alpha t \right\}.$$

In the case of a point source in an infinite media, the

temperature at a point of coordinates x, y, z , at time t , is obtained by integrating the previous equation, giving:

$$S_p = \frac{Q_p}{4\pi K r} \operatorname{erfc}\left[r/(4\alpha t)^{1/2}\right], \tag{6}$$

where Q_p is the power of the point source, independent of time; K is the conductivity in the media; and r is the distance between the point under consideration and the source; erfc is the complementary error function. This result cannot be applied if the source decays with time. However, it may be useful when accuracy is studied for the technique introduced here.

When the source is linear and independent of time, the non-stationary solution for large values of t (for all practical purposes, the values of t are of the order of several years) is:

$$S_t = \frac{Q_1}{4\pi K} \left[\ln\left(\frac{4\alpha t}{r^2}\right) - \gamma \right],$$

where Q_1 is the linear power density and γ is Euler's constant (≈ 0.577).

The steady solution takes the following form:

$$S_1 = \frac{Q_1}{2\pi K} \ln(r/L),$$

where L is a constant of characteristic length.

When sources are variable with time, the solution may be obtained by means of numerical techniques. This is still true for very simple cases, such as the ones shown above, although for the latter the techniques shown here are economical as far as computational costs are concerned.

Beyerlein and Clairborne [4] summarized a set of equations for sources of interest for the case in which source decay may be shown as:

$$Q = Q_0 A \exp(-\lambda t).$$

In this case, the solution corresponding to the point source is:

$$S_p = \frac{A e^{-r^2/4\alpha t}}{4\pi K} R\left[\lambda, t, r/(4\alpha t)^{1/2}\right], \tag{7a}$$

where R is the real part of the complex-argument error function, defined as:

$$W(c) = e^{-c^2} \left(1 + \frac{2i}{\pi} \int_0^c e^{-t^2} dt \right) \equiv e^{-c^2} \operatorname{erfc}(-ic).$$

For the case of a plane source, the solution is:

$$S_{PL} = \frac{A\alpha}{2K\lambda} e^{-z^2/4\alpha t} J\left[(\lambda t)^{1/2}, z/(4\alpha t)^{1/2}\right], \tag{7b}$$

where J is the imaginary part of $W(c)$ and where, additionally, it has been assumed that the source is located at the origin of the coordinates ($z = 0$).

When the sources have a finite length, the solutions may be obtained from numerical quadratures, even in the case of a constant power.

The equation corresponding with a $2L$ -long finite source parallel to the x axis is

$$S_1 = \int_0^t \frac{Q(t')}{8\pi\alpha} \left(\operatorname{erfc}\left(\frac{(x+L)}{[4\alpha(t-t')]^{1/2}}\right) - \operatorname{erfc}\left(\frac{(x-L)}{[4\alpha(t-t')]^{1/2}}\right) \right) \exp\left\{-\left[(y-y')^2 + (z-z')^2/4\alpha(t-t')\right]\right\} \frac{dt'}{(t-t')}. \tag{8}$$

as shown by Tin Chan et al. [14]. Since the subintegrand of this equation has some special features, it may be subdivided into areas, as shown in ref. [2], although experience showed later that this was unnecessary.

A similar treatment may be applied to the case of a plane source with finite dimensions. In this case eq. (8) would become:

$$S_{PL}(x, y, z, t) = \frac{\alpha}{8K(\alpha\pi)^{1/2}} \int_0^t \frac{Q_p(t-\mu)}{\mu} \times F_1 F_2 e^{-z^2/4\alpha\mu} d\mu, \tag{9}$$

with

$$F_1 = \operatorname{erf}\left(\frac{x+M}{2(\alpha\mu)^{1/2}}\right) - \operatorname{erf}\left(\frac{x-M}{2(\alpha\mu)^{1/2}}\right) \tag{10a}$$

and:

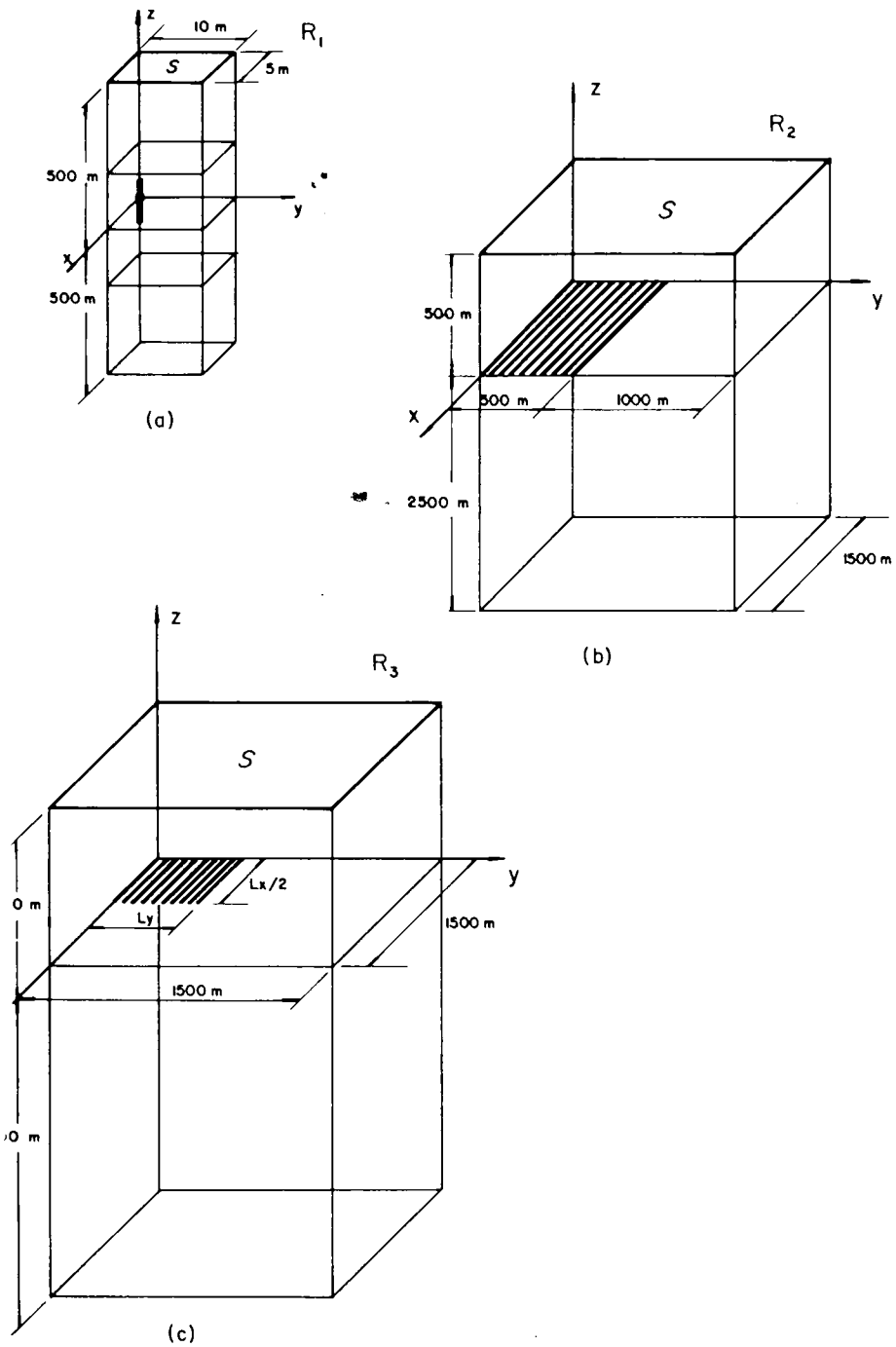
$$F_2 = \operatorname{erf}\left(\frac{y+N}{2(\alpha\mu)^{1/2}}\right) - \operatorname{erf}\left(\frac{y-N}{2(\alpha\mu)^{1/2}}\right), \tag{10b}$$

where $\mu = t - t'$.

Details on this solution cannot be found in the literature. Therefore, the complete results will be considered separately.

While the equations shown refer to an infinite media, interest in this case is centered upon a semi-infinite media. This may be solved by means of the image method, which is valid for the linear case.

The details of the calculations performed are shown further on in this paper.



2. Domains of integration under consideration.

4. Preliminary numerical studies

In order to attain a proper idea of the accuracy of the results, some studies and comparisons with previous results were performed so as to verify the influence of the boundary conditions upon the same.

Unless stated, the values of the transport parameters were representative of those encountered in a typical granite mass, i.e., $K = 2.58$ kcal/m/h/°C, $\rho C = 520$ kcal/m³/°C. The heat source was also representative of a typical thermal load [10] namely 430 kcal/h.

For almost every case, the geothermal gradient was considered as imposed, resulting in $T_S = 15.3^\circ\text{C}$ for $z = 500$ m and in $T_0 = 32^\circ\text{C}$ for $z = 0$. The influence of the flux-type boundary condition was found to be negligible by Ratigan [12] for the usual values of the heat transfer coefficients and, therefore, it will not be considered further. The imposed geothermal gradient was $1^\circ\text{C}/30$ m.

Fig. 2 shows three integration domains, R_i , $i = 1, 2, 3$. Domain R_1 is representative of that previously considered by the authors [16], consisting of a unit cell with a container. Domain R_2 represents the case considered by Ratigan [12] and later by Rae and Robinson [11]. Domain R_3 represents an idealization of the thermal load (rectangle ABCD in fig. 1) and of the surrounding media for a case of our interest, Palacios et al. [10] which will be discussed further on in this paper.

The various versions of the program developed allowed for a correct treatment of some problems of interest. Almost all cases were considered as 3D, under adequate boundary conditions and ad hoc sources, so as to simulate 2D cases (domain R_2).

Let us first consider the previous results obtained

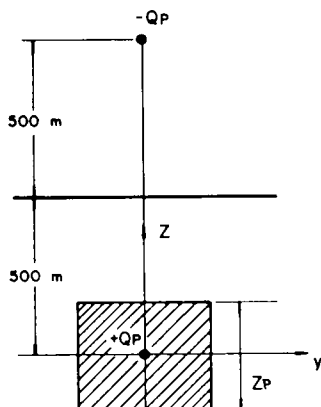


Fig. 3. Unit cell for the verification of the boundary-condition effect.

with domain R_1 . One of the developed versions allowed for considering constant-spacing areas that partially represented the phenomenon, with a steady point source. This has been illustrated in fig. 3 for plane $x = 0$. For the sake of clarity, the figure shows the symmetric source that allows for a representation of the surface.

The results obtained from different versions of the code using variable and constant grids were compared with each other and the results of the comparison are shown in fig. 4. The shaded zone of fig. 3 was divided into a regular grid of $10 \times 10 \times 20$ points in the x , y , z directions, respectively. The width of the zone was 20 m along x and y , and the height of the integration sub-domain (ZP) was varied to consider the influence of boundary conditions as time elapsed. The boundary conditions were adiabatic in the vertical walls and implied fixed temperatures (coincident with the geother-

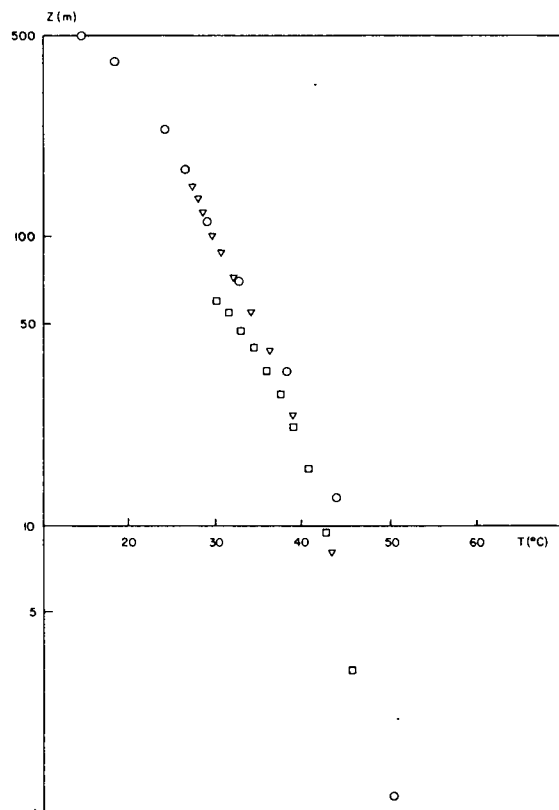


Fig. 4. Influence of the boundary conditions upon the results; $x = y = 1.1$ m, $t = 50$ y and $Q = 500$ W;
 ○ variable grid, $\Delta t = 0.25$ y.
 ▽ constant grid ($ZP = 300$ m), $\Delta x = \Delta y = 1.1$ m; $\Delta z = 15.8$ m;
 □ constant grid ($ZP = 120$ m), $\Delta x = \Delta y = 1.1$ m; $\Delta z = 6.3$ m.

distribution) at the top and at the bottom. The one resulting from $ZP = 120$ m and from a uniform distribution of 20 points demonstrated that it was not convenient to work with portions of the area of interest, because – as time went by – there was an increase of the influence of the repository upon the temperature distribution, involving larger and larger areas of the rocks. For $t < 50$ y, the height $ZP = 300$ m was safe, as a boundary condition. Another set of calculations was formed employing a graded mesh defined by $Z(i) = ZP \{ [(i - 1) ZP/19 - ZP/2]/ZP \}^2 \text{ sign}(k - 11)$ for $ZP = 1000$ m. This mesh avoids the origin where the steady point source is located and varies parabolically with the distance to the origin. The results obtained are shown as circles in fig. 4 and served to check the sensitivity of the codes with respect to grid divisions. Calculations were performed with $\Delta t = 5$ y.

Comparisons were made for a one-dimensional case with spherical symmetry involving a point source. The case was treated as Cartesian, as from a transformation

$T' = Tr$, where T' is the “temperature” in the Cartesian case. The geometrical dimensions and the physical features of the source, as well as the materials, corresponded to the actual case and are shown in fig. 5. The source was constant in time, selecting $\Delta t = 0.5$ y, and the integration was extended to 10^4 y. The grid was variable, with 10 points on the r axis located at $r = 5, 15, 30, 60, 130, 200, 350, 500, 750$ and 1000 m. The results for $t = 50$ and 10^4 y are shown in the same figure. Errors, with respect to eq. (7a) are shown on the right side of fig. 5 and, for $t = 10^4$ y, they did not surpass 0.5% in the areas of interest. Naturally, errors increased up to 2%, as T decreased to 5×10^{-2} .

The geometry shown in fig. 2b was used for comparison between our results and those obtained by Ratigan [12]. The continuous source of such a reference was simulated for cases with and without decay. The latter case was included among those considered by Rae and Robinson [11].

Both references show calibration results against a one-dimensional case involving the consideration of a

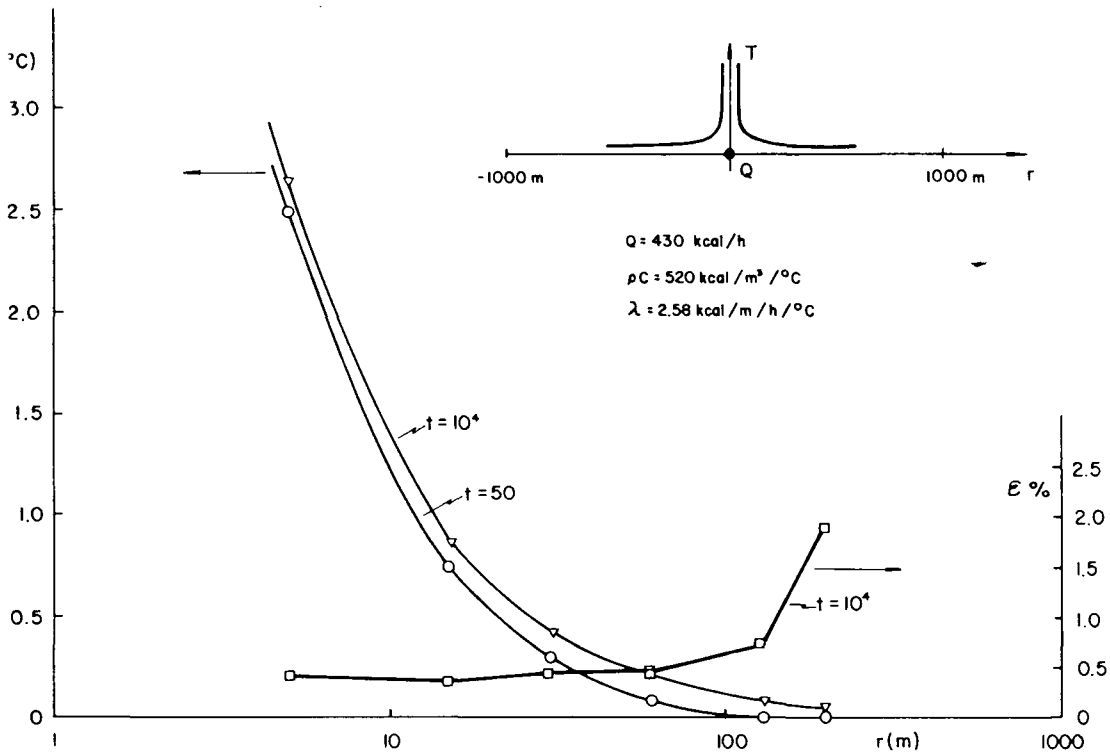


Fig. 5. Comparison of numerical and analytical solutions (radial symmetry case). — analytical solution; symbols: numerical solutions; t in years and $\Delta t = 0.5$ y.

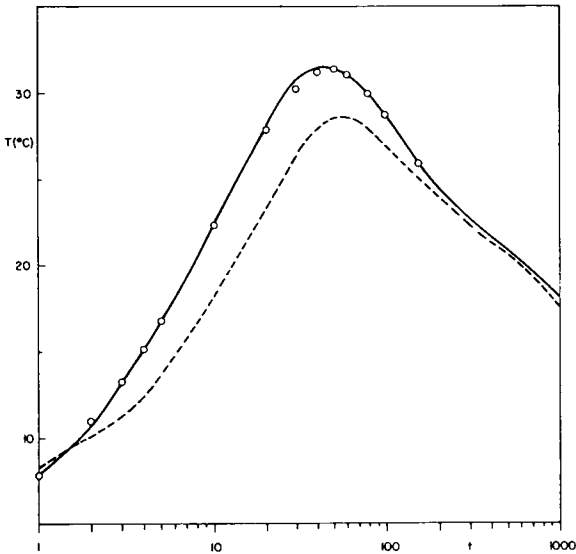


Fig. 6. Comparison with Ratigan's results [12], decaying source, one-dimensional simulation, $x = y = z = 0$; $\Delta t = 0.5$ y. — analytical solution; - - - Ratigan [12]; \odot present; t in years.

continuous plane source. The source is finite in both cases and the results were compared, for control purposes, with those obtained from the infinite source. Results were obtained employing a graded grid with $12 \times 12 \times 20$ points and $\Delta t = 0.5$ y. This grid simulated the corresponding one in Ratigan's work [12], whose results approximate the temperature at the repository plane, as indicated in fig. 6, where the results of the analytical solution (eq. (7b)) are also included. The circles serve to indicate the results obtained from the technique considered here and are consistent with the one-dimensional approach under analysis. Rae and Robinson [11] showed a slightly better comparison than Ratigan between their results and the analytical ones.

Fig. 7 shows, for plane $z = 0$, a comparison between our results and those obtained by Rae and Robinson [11] for the source with decay and under a one-dimensional approach. As may be seen, this is an excellent comparison and there is coherence with what is shown in fig. 5. The same grid and time step were used as before.

Comparisons were also performed with previous results obtained by the authors for the case of the domain shown in fig 2a. In this case, two types of sources were considered, corresponding to a point source and to a finite linear source. In both cases, the boundary condi-

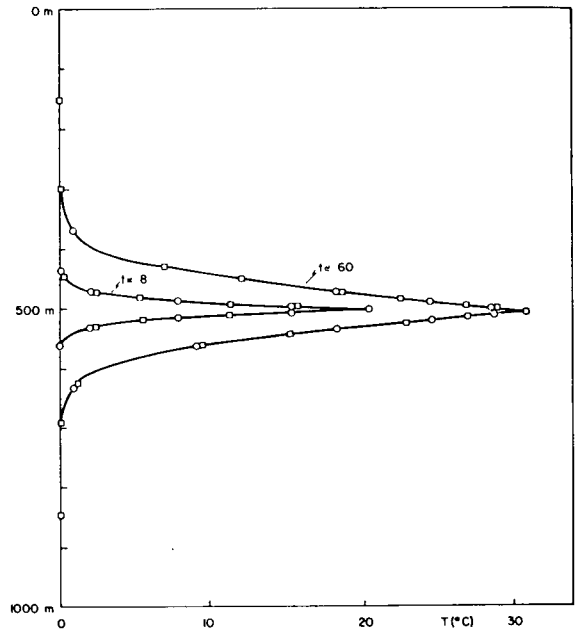
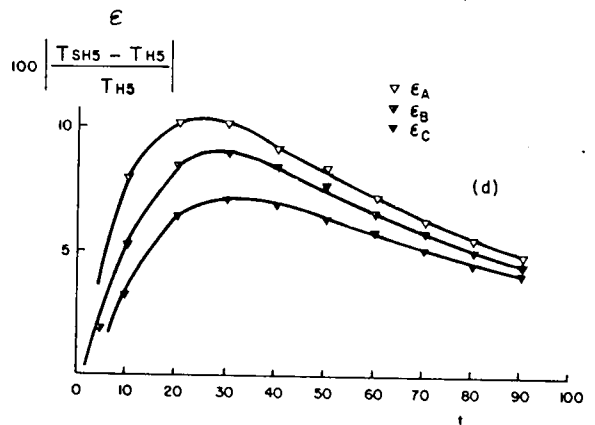
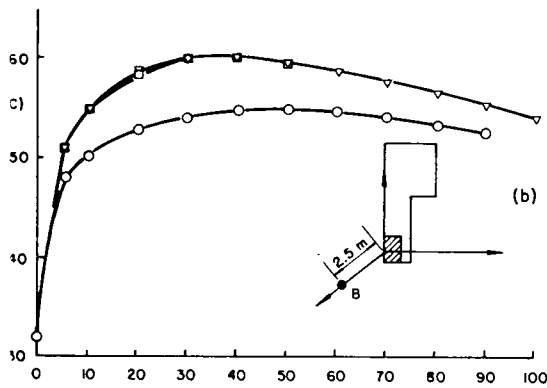
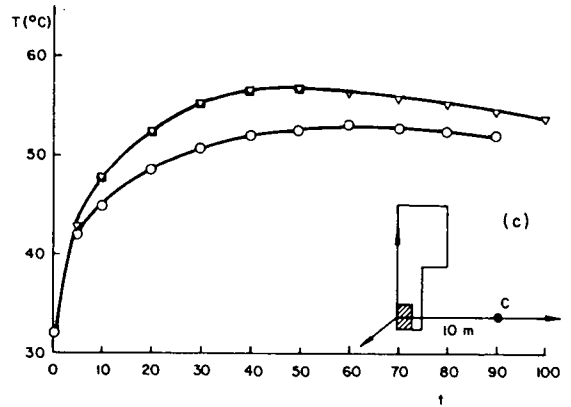
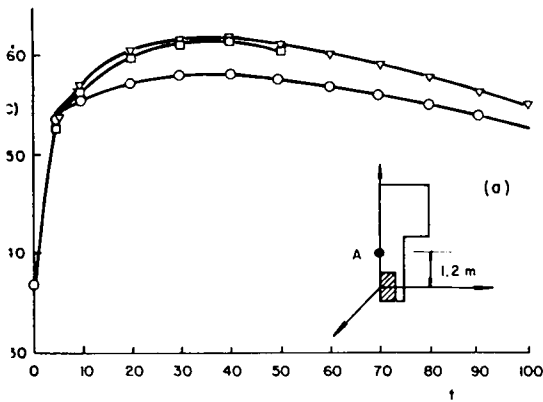


Fig. 7. Comparison with Rae and Robinson's results [11], decaying plane source, one-dimensional simulation, $x = y = 0$; $0 \leq z \leq 1000$ m; $\Delta t = 0.5$ y. — analytical solution; \square Rae and Robinson [11]; \odot present; t in years.

tions coincided with those previously shown by the authors [16]; that is, they were adiabatic at the vertical walls and the temperature was constant at the earth's surface and at 2000 m deep.

Fig. 8 shows a comparison between the results obtained by the Heating 5 code, see Turner et al. [15], and by the technique introduced here for three points of interest, representatives of a pillar between galleries, of the center between two containers and of a point on a container axis. Only five nodes were considered as per directions x and y , while 20 nodes were considered along z . The time step was 0.5 y. The calculations were performed without considering the symmetry of the system and using the results of Heating 5 (shown as H5 in fig. 8) as a reference. Differences hardly went over 10%, tending to decrease with time, and stabilize at 5% as a whole. If the discretization used is taken into account, the results compare excellently with those considered as basic (H5). On the other hand, the differences in the composition of the media, that were considered in the base case, were disregarded in our model. The codes developed showed almost the same performance when consideration was given to the so-called "grind time" (i.e., CPU time/number of cells/number of time steps).



In fact, this time was 0.0067 and 0.0059 s/cell/time step for the H5 calculations and for our calculations, respectively, (12% gain) with the point source in an IBM 70/158 computer. Furthermore, we can increase grid dimensions (and, correspondingly, the time steps) without any significant loss of accuracy, thus allowing accurate calculations in large regions. The authors' idea is not to consider these programs as "superior" than HEATING 5. The intention is to show that it is possible to use a particular technique advantageously in this case.

As a last verification step and considering the need to acquire some experience on the simulation of continuous sources, the two-dimensional configuration issued by Ratigan [12] was represented, considering 51 year sources (and their images). The sources were considered to have a length equal to that of the integration domain in the sense x (see fig. 2b), that is 1500 m, and were separated at a distance, L_f , of 10 m in order to cover 500 m as indicated by Ratigan [12]. The rest of the dimensions were adjusted as shown in fig. 2b. The number of nodes, as per coordinate y , was 10 (half of those in the quoted reference).

Fig. 8. Comparison between calculations made through the use of the HEATING 5 code and the present technique. \circ HEATING 5; ∇ present (point source); \square present (finite linear source); t in years.

Results were simulated as if corresponding to sources without decay (shown by Rae and Robinson [11]), as well as for cases with radioactive decay, both with the same programme.

Fig. 9 shows an excellent comparison with the results obtained by Rae and Robinson [11] for the case without decay.

Fig. 10 is a comparison for the case of sources with decay. This was only performed for a period of ten years, with $\Delta t = 0.5$ y, since the computational cost was considered as excessive for a test. The comparison is also good and fig. 11 shows a temperature profile along the repository plane. The difference with the previous data does not exceed 3% and the authors believe it is due to the small local differences in modelling the sources.

The results shown above indicate that the technique developed is attractive and reliable, while comparable

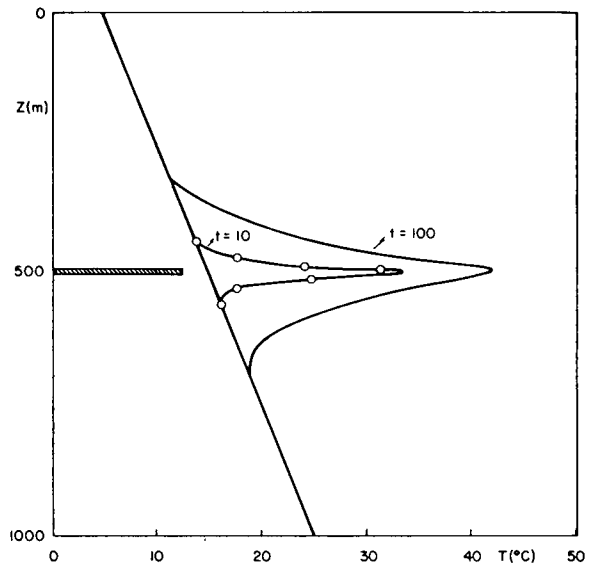
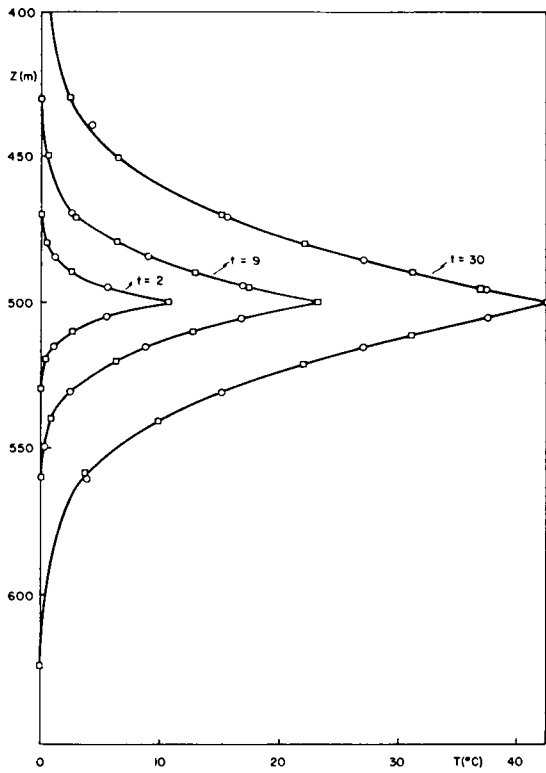


Fig. 10. Comparison with Ratigan's results [11], decaying sources, z axis. — Ratigan [12]; \odot present; t in years.

Fig. 9. Comparison with Rae and Robinson's results [11], constant sources, simulation by means of linear sources, z axis. — analytical solution; \square Rae and Robinson [11]; \odot present; t in years.

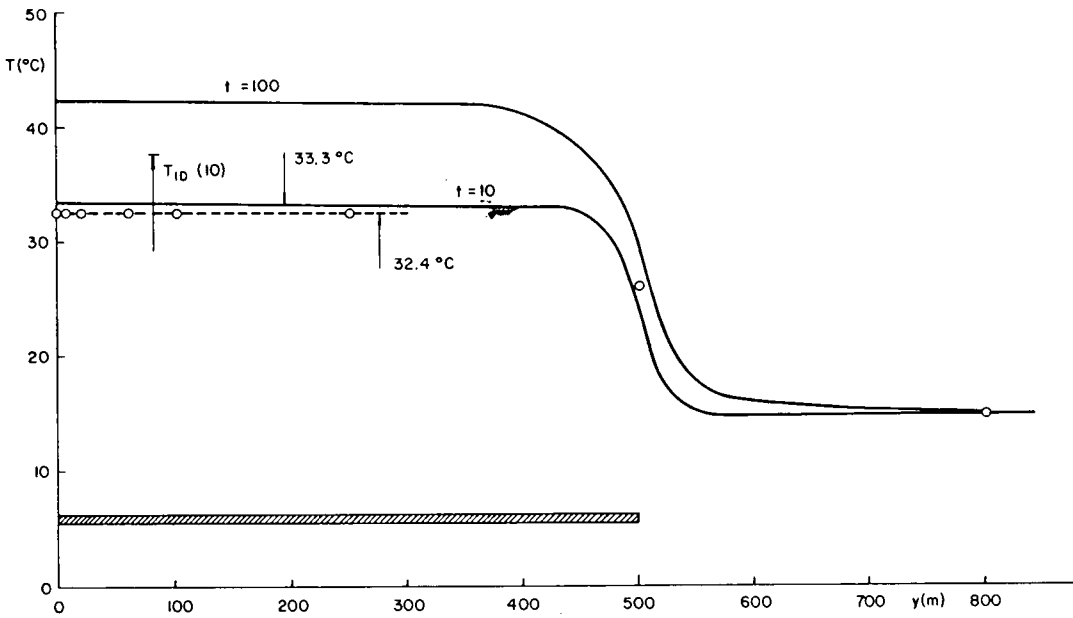
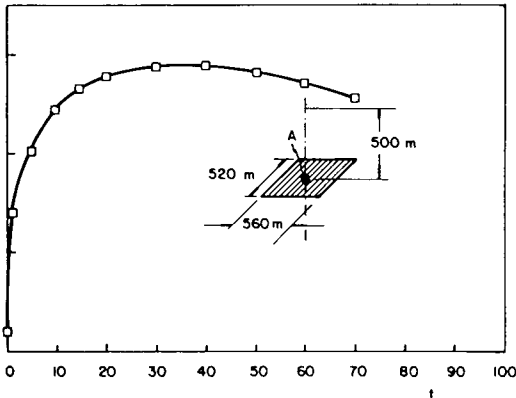


Fig. 11. Temperature profile along the repository, $x = z = 0$; $\Delta t = 0.5$ y. — Ratigan [12]; \odot present; t in years.

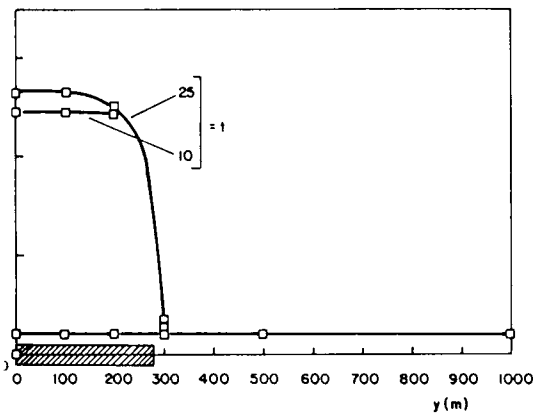


2. Temperature time evolution for point A ($x = y = 0$, $z = 1$). Simulation by means of linear sources; t in years.

those in the consulted literature. This is coherent with the indications made by Emery [7] for simpler

Application in a typical repository

A basic study case of the repository consists in a geometry like that indicated in fig. 2c. L_x and L_y are defined in such a way that the total number of containers (N_c), estimated as 3000, may be installed in series running at $D_p = 20$ m from each other and at 5 m from each other. Considering a total of 29 containers, with a total length $L_x \approx 520$ m, 3046 containers may be lodged in a plant of 0.29 km^2 . This



13. Temperature time evolution along axis y . ($z = 1$); t in years.

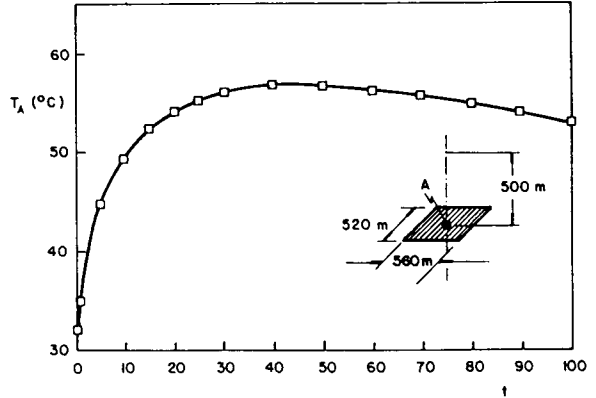


Fig. 14. Temperature time evolution in the repository plane. Point A ($x = y = z = 0$). Simulation by means of a continuous plane source. t in years.

implies a thermal load of 5200 kW/km^2 (5.2 W/m^2), if each container has an initial power of 500 W.

Results were obtained for a case of sources with decay for a law of the type

$$Q = Q_0 \exp(-2.28 E - 6t),$$

where t is given in hours. This variation is an approximation to the decay of wastes resulting from the reprocessing of nuclear fuel.

The results were obtained by means of a coarse grid, with $8 \times 8 \times 14$ nodes in directions x , y and z respectively. As per the considerations made in the previous section, this grid ensures a reasonable accuracy in the results. Besides, consideration was given to the symme-

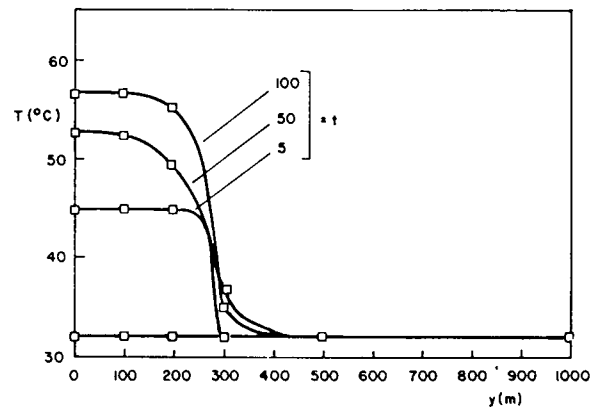


Fig. 15. Temperature time evolution in the repository plane along axis y . ($z = x = 0$); t in years.

try of the system. Calculations were performed with $\Delta t = 0.5$ y.

Fig. 12 shows the temperature–time evolution at the repository axis ($x = 0$, $y = 0$, z) while fig. 13 shows the temperature variation for $z = 1$ m and $x = 0$. The variation along z looks similar.

Simulations were also performed for results from a finite plane source equivalent to the repository. The results may be seen in fig. 14 and 15, showing identical tendencies to those in figs. 12 and 13. The latter way of simulating the repository is highly economical in computation time and, therefore, it will be used in performing future parametric studies.

The differences in the results are only apparent, since they are actually local effects of the various sources. Thus, the comparison of both cases, for $z = 20$ m and for $x = y = 0$, shows a difference that is not above 2%.

6. Conclusions

Results were obtained concerning heat transfer in an isotropic semi-infinite media involving concentrated sources for heat generation. These sources may be considered as generators of temperature boundary layers. This implies that a standard approximation to the finite differences will require severe computational costs, so as to reach a reasonable accuracy.

In order to solve the above difficulty, a technique was considered allowing for an adequate treatment of sudden variations in temperature, which was applied by Emery [7] and whose general formulation is shown in Appendix A.

As from a computational viewpoint, a distribution of pseudo-sources was applied, as a representation of the concentrated sources. This was combined with the linear version of an implicit algorithm with alternating directions as described by Ventura et al. [17]. In the version introduced here, the logic may be simply altered in order to consider different types of sources.

The results show an excellent comparison with calibration cases and allow us to assume their validity in the other cases under consideration.

Thus, a valuable technique has been applied to this type of study, since it has the following advantages: it has no precision problems connected with the presence of isolated singularities, the number of nodes in the grid is reasonable (of the order of 2000) for the 3D cases, the data structure leads to tridiagonal schemes, the grid is variable and the technique is unconditionally stable. Finally, disadvantages are related with the time needed to calculate the local analytical solutions; however, for

those cases in which we are interested, this has allowed for a quite detailed simulation of the local temperature peaks.

Additionally, this technique is considered particularly important as far as design is concerned, since it also allows for an adequate simulation of the thermal history in terms of the filling of the repository. This can naturally be extended to other applications.

A simply way was also considered for the representation of the repository. This consisted in the integration of a finite, plane heat source with a rectangular plant. This representation has been shown to be reliable when compared with one dimensional cases and, therefore, it will be employed for the application of the model in cases of interest. However, it only allows for approximately simulating a progressive filling of the repository.

Acknowledgements

The helpful comments of Professor S.W. Churchill and of the referees, which improved the paper, are gratefully acknowledged by the authors.

Appendix A. Consideration of singularities in the finite difference method

The fact that the presence of singularities in an integration domain or in its boundary introduces difficulties for its numerical resolution is well known. Fox [18] summarized the usual techniques for the treatment of these problems. These are generally ad-hoc techniques for different cases.

Emery [7] introduced another working technique that is valid for the case of finite differences and finite elements, consisting in generating a pseudo source distributed all over the field, representing the influence of the perturbation caused by the isolated “singularity(ies)”. The case dealing with finite differences will be the one considered in this Appendix in a broader sense than that originally considered by Emery [7], although based on the same concepts. “Singularities” are very strong variations of the variables of interest. We have preferred to maintain a vague sense in the definition of the same, although, in the case of stationary sources, those are singularities in the analytical sense of the word.

Let us consider that the problem to be solved is the following:

$$OT + Q + \sum_i q_i = 0, \quad (A1)$$

$\nabla \cdot \mathbf{O}$ is the differential operator, T is the temperature, \mathbf{Q} are the distributed sources and q_i are the concentrated sources.

Consideration will only be given to the case in which the intensity of the sources is known. Therefore, no materials will have to be assessed and there will be no complexities associated with the boundary conditions. It will be considered [7] that the solution to eq. (A1) can be shown as follows:

$$\nabla \cdot \sum_i S_i, \tag{A2}$$

The subscript h serves to indicate a discrete version of the operator, S represents the analytical solution to the problem:

$$q_i = 0, \tag{A3}$$

the temperature showing a smooth variation within the integration domain. Then,

$$\nabla \cdot \mathbf{O}_h \bar{T} + \mathbf{O}_h S. \tag{A4}$$

If T is smooth, then $\mathbf{O}_h T$ is a good approximation; therefore,

$$\nabla \cdot \mathbf{O} \bar{T} = \mathbf{O} T - \mathbf{O} S = \mathbf{Q}.$$

$$\nabla \cdot \mathbf{Q} - \mathbf{O}_h S = 0. \tag{A5}$$

If $\nabla \cdot \mathbf{Q} = 0$ and $\mathbf{O} \equiv \nabla^2$, then eq. (A5) is the equation derived by Emery [7] for steady problems. When:

$$\frac{\partial}{\partial t} - \alpha \nabla^2,$$

we are dealing with the case that Emery [7] considered for time-dependent problems (note that the sources may be constant with time).

References

1. K. Althofen, Waste package heat transport analysis, Lockheed International Corp., Richland, WA, USA., DOE-BWI-ST-18 (October 1981).
 2. Anonymous, Thermal operations conditions in a national waste terminal storage facility, Science Applications INC., DOE/OWI/SUB-76/47950 for the Office of Waste Isolation, DOE (September 1976).
 3. V.M. Kays, F. Hossaini-Hoshemi and J.S. Bosch, Calculations of media temperatures for nuclear sources in geologic

repositories by a finite-length line source superposition model (FLLSSM), Nucl. Engrg. Des. 67 (1981) 339-347.
 [4] S.W. Beyerlein and H.C. Clairborne, The possibility of multiple temperature maxima in geologic repositories for spent fuel from nuclear reactors, ORNL/TM-7024 (1979).
 [5] H.C. Clairborne, R.S. Wagner and R.A. Just, A comparison of the results of several heat transfer computer codes when applied to a hypothetical nuclear waste repository, ORNL/TM/7112 (December 1979).
 [6] H.S. Carslaw and J.C. Jaeger, Conduction of Heat in Solids (Clarendon Press, Oxford, 1959).
 [7] A.F. Emery, The use of singularity programming in finite-difference and finite-element computations of temperature, ASME Trans., J. Heat Transfer 95 (1973) 344-351.
 [8] L. Fox, in: A Survey of Numerical methods for Partial Differential Equations, eds., I. Gladwell and R. Wait (Oxford University Press, 1979).
 [9] G.I. Marchuk, Methods of Numerical Mathematics, (Springer Verlag, Berlin, 1975).
 [10] E. Palacios, J. Mattar, C. Perucca and G.E. Preisz, Bases conceptuales para la construcción de un repositorio en la Argentina, IAEA-CN-43/439, Int. Conf. on Radioactive Waste Management, Seattle, WA, USA (1983).
 [11] J. Rae and P.C. Robinson, NAMMU: Finite element program for coupled heat and groundwater flow problems, AERE-R 9610, Theoretical Physics Div., AERE Harwell, Oxfordshire (November 1979).
 [12] J. Ratigan, Groundwater movements around a repository; Thermal analysis: Part 1 Conduction Heat transfer, Part 2: Advective heat transfer, KBS Rept. 54:02 (1977).
 [13] R.M. Thunvik, Hydrothermal conditions around a radioactive waste repository, Parts I, II and III, KBS Rept. 80-19 and 82-01 (1980-1981).
 [14] Chan Tin, G.W. Neville and Tsang Chin-Fu, Theoretical temperature fields for the Stripa Heater Project, vol. 1, LBL-7082 (September 1978).
 [15] W.D. Turner, D.C. Elrod and I.I. Simanton, Heating 5, An IBM 360 heat conduction program, OAK RIDGE Nat. Lab., ORNL/CSD/TM-15 (1977).
 [16] M. Ventura and J.C. Ferreri, Evolución temporal de un macizo granítico bajo cargas térmicas generadas por productos de fusión, Parte a: estudio básico, parte b: estudio Paramétrico, Gerencia de Protección Radiológica y Seguridad, CNEA (1982).
 [17] M. Ventura, R. Rosso and J.C. Ferreri, Further application of CODIF: three-dimensional scalar transport with second order reaction, Lat. Am. J. Chem. Eng. Appl. Chem. 8 (1978) 73-77.
 [18] J.S.Y. Wang, C.F. Tsang, N.G.W. Cook and P.A. Witherspoon, A study of regional temperature and thermohydrologic effects of an underground repository for nuclear wastes in hard rock, J. Geophysical Res. 86 (1981) 3759-3770.